JOURNAL OF SOLID STATE CHEMISTRY 15, 274–282 (1975)

Structural Studies in the Li_2MoO_4–MoO_3 System: Part 2. The High-Temperature Form of Lithium Tetramolybdate, *H*-$Li_2Mo_4O_{13}$

B. M. GATEHOUSE AND B. K. MISKIN

Chemistry Department, Monash University, Clayton, Victoria, Australia, 3168

Received November 20, 1974

H-$Li_2Mo_4O_{13}$ crystallizes in the triclinic space group, $P\bar{1}$, with cell parameters $a = 8.612$ Å, $b = 11.562$ Å, $c = 8.213$ Å, $\alpha = 94.45°$, $\beta = 96.38°$, $\gamma = 111.24°$, and $Z = 3$. The structure was solved using three-dimensional Patterson and Fourier techniques. Of the 4403 unique reflections collected by counter methods, 2883 with $I > 3\sigma(I)$ were used in the least-squares refinement of the model to a conventional R of 0.031 ($R_w = 0.035$). Like *L*-$Li_2Mo_4O_{13}$, *H*-$Li_2Mo_4O_{13}$ is a derivative structure of V_6O_{13} and can be related to *L*-$Li_2Mo_4O_{13}$ by movement of one of the shear planes in the structure.

Introduction

Brower et al. (*1*) reported the existence of the dimorphs of lithium tetramolybdate, *L*- and *H*-$Li_2Mo_4O_{13}$. Gatehouse and Miskin (*2*) reported the crystal structure of the *L*-form, which was shown to be a regular derivative structure of V_6O_{13} (*3*, *4*). As the following report shows, *H*-$Li_2Mo_4O_{13}$ is also a regular derivative structure of V_6O_{13} and bears an interesting relationship to the low-temperature form.

Experimental

A small sample of *H*-$Li_2Mo_4O_{13}$, prepared by heating the appropriate ratio of Li_2MoO_4 and MoO_3 for 18 hr in a sealed Pt tube at 547°C, was kindly supplied by Roth (*1*). The pale green crystals were small and had poorly defined external morphology. Preliminary Weissenberg photography indicated that the structure of *H*-$Li_2Mo_4O_{13}$ would bear a strong resemblance to that of the low-temperature form and yielded cell parameters of sufficient accuracy to enable the subsequent alignment of a crystal on the diffractometer. Due to insufficient sample, the density of the compound was not measured, but since the cell volumes of the *H* and *L* forms were the same it was assumed that Z would be the same for both; i.e., $Z = 3$.

A small, irregular crystal (0.03 × 0.03 × 0.06 mm) was mounted about the longest dimension (*a*-axis) and aligned on a Picker Nuclear FACS 1 four-circle automatic diffractometer (by courtesy of Dr. G. B. Robertson, Research School of Chemistry, Australian National University, Canberra). All data were collected using graphite monochromated MoK_α radiation. A least-squares refinement of cell and orientation parameters using 12 high-angle reflections gave the cell dimensions reported in Table I.

Intensities were collected by θ–2θ scans with a scan width ($\Delta 2\theta$) of 1.3° and allowance for spectral dispersion. Background counts of 10 sec duration were measured at both the upper and lower limits of the scan. The intensities of three noncoplanar reference reflections monitored after every 50 reflections showed no systematic variation throughout the period of data collection. All 4403 unique reflections with $3° \leqslant 2\theta \leqslant 60°$, $|h| \leqslant 11$, $|l| \leqslant 18$ and $0 \leqslant k \leqslant 11$ were collected, although the 1520 reflections with intensity $I \leqslant 3\sigma(I)$ and uneven backgrounds $[|B_1 - B_2| \geqslant 3\sigma(B_1 + B_2)]$ were given zero weight in the structure solution and refinement.

TABLE I

CRYSTALLOGRAPHIC DATA FOR H-$Li_2Mo_4O_{13}$[a]

Symmetry: triclinic; space group: $P\bar{1}$	
a: 8.612(4) Å	α: 94.45(7)°
b: 11.562(6) Å	β: 96.38(7)°
c: 8.213(4) Å	γ: 111.24(7)°
V: 751(1) Å^3	Z: 3
D_c: 4.01(1) g cm^{-3}	μ_c(MoK_α): 48.63 cm^{-1}

[a] Estimated standard deviations are in parentheses.

The intensities were corrected for Lorentz and polarization effects and reduced to observed structure amplitudes. Since the plane of reflection of the monochromator crystal was perpendicular to that of the specimen, the Lorentz polarization correction was

$$(Lp)^{-1} = \sin 2\theta(1 + \cos^2 2\theta_m) / (\cos^2 2\theta_m + \cos^2 2\theta),$$

where $\theta_m = 6.00°$ was the Bragg angle of the monochromator. The variance of the structure amplitude, F, was calculated as

$$\sigma^2(F) = [(C + \tau^2 B) + 0.001I^2]/[2F(Lp)]^2,$$

where C is the peak count, B is the sum of the two background counts, τ is the ratio of count time to background time, and I is the net intensity $(C - \tau B)$. Since μR was of the

TABLE II

FINAL POSITIONAL PARAMETERS (×10^4) AND TEMPERATURE FACTORS FOR H-$Li_2Mo_4O_{13}$[a]

(a) Atoms with anisotropic temperature factors

Atom	x	y	z	U_{11}	U_{22}	U_{33}	U_{12}	U_{13}	U_{23}
Mo(1)	3454(1)	3650(1)	254(1)	61(4)	69(4)	54(4)	18(3)	10(3)	−1(3)
Mo(2)	3272(1)	3638(1)	4157(1)	51(4)	73(4)	56(4)	22(3)	10(3)	15(3)
Mo(3)	3048(1)	6385(1)	6240(1)	61(4)	87(4)	69(4)	42(3)	7(3)	7(3)
Mo(4)	3206(1)	6332(1)	2282(1)	70(4)	84(4)	63(4)	41(3)	14(3)	15(3)
Mo(5)	1469(1)	9665(1)	3661(1)	78(4)	91(4)	72(4)	40(3)	13(3)	17(3)
Mo(6)	1639(1)	9643(1)	9705(1)	79(4)	94(4)	74(4)	47(3)	9(3)	5(3)

(b) Atoms with isotropic temperature factors

Atom	x	y	z	B	Atom	x	y	z	B
O(1)	0	0	5000(0)	1.14(17)	O(13)	13(9)	9918(7)	1532(9)	0.99(12)
O(2)	6724(10)	9932(8)	4933(10)	1.42(13)	O(14)	2887(9)	9971(7)	1875(10)	1.00(12)
O(3)	1858(9)	6133(7)	4060(9)	0.77(11)	O(15)	6735(10)	9982(8)	1415(10)	1.44(14)
O(4)	4641(9)	5989(7)	4396(9)	0.72(11)	O(16)	1448(10)	5972(8)	833(10)	1.26(13)
O(5)	7843(9)	5841(7)	4500(9)	0.97(12)	O(17)	4619(9)	5810(7)	884(9)	0.85(11)
O(6)	2377(10)	2062(7)	3887(10)	1.19(12)	O(18)	8050(10)	6183(7)	1115(9)	1.04(12)
O(7)	6185(11)	2037(8)	3428(11)	1.52(14)	O(19)	2875(10)	2076(7)	1553(10)	1.10(12)
O(8)	651(11)	8083(8)	3435(11)	1.68(14)	O(20)	9217(11)	1943(8)	608(11)	1.60(14)
O(9)	4187(10)	7887(7)	2461(10)	1.41(13)	Li(1)	9909(27)	3708(20)	1046(27)	1.5(3)
O(10)	2346(9)	4095(7)	2153(9)	0.69(11)	Li(2)	5200(30)	38(22)	2944(30)	1.9(4)
O(11)	5106(9)	3896(7)	2556(9)	0.77(11)	Li(3)	9679(27)	6243(20)	3087(27)	1.6(4)
O(12)	8578(10)	4111(7)	2624(10)	1.29(13)					

[a] Estimated standard deviations are in parentheses. B is the Debye–Waller temperature factor and the anisotropic temperature factor is of the form:

$$\exp[-2\pi^2(U_{11}h^2a^{*2} + U_{22}k^2b^{*2} + U_{33}l^2c^{*2} + 2U_{12}hka^*b^* + 2U_{13}hla^*c^* + 2U_{23}klb^*c^*) \times 10^{-4}].$$

order of 0.1, no correction for absorption was applied to the data.

The scattering factor curves used in the structure factor calculations were those of Cromer and Waber (*5*) for Mo^0, O^0 and Li^+. All computing was performed on the Monash University CDC 3200 and CSIRO CDC 3600 computers. The major programs used were MONLS, a modified version of the full-matrix least-squares program of Busing, Martin, and Levy (*6*); MONDLS, a block-diagonal least-squares program adapted from the "SF" series of programs by Shiono (*7*); and MONFR, the Fourier summation program of White (*8*).

Structure Solution and Refinement

The structure was solved using the method described by Gatehouse and Leverett (*9*). Twelve molybdenum positions were readily found and an examination of this model revealed a center of symmetry. In addition, a difference electron density map contained a large number of peaks which could be taken as oxygen positions. Full-matrix least-squares refinement of the centrosymmetric model with all six molybdenum positions and the 10 oxygen positions which were unambiguously located resulted in a conventional residual

$$R = \sum \| F_o| - |F_c\| / \sum |F_o|$$

of 0.25. The remaining 10 oxygen positions were located in a difference Fourier synthesis and successive cycles of refinement of the positional parameters for the complete Mo–O model—with the exception of those for O(1), which was located at a center—reduced R to 0.068.

With "observed" reflections weighted by $1/\sigma^2(F)$, three cycles of block-diagonal least-squares refinement of positional and isotropic thermal parameters reduced R to 0.047 and the weighted residual

$$R_w = (\sum w(|F_o| - |F_c|)^2 / \sum wF_o^2)^{1/2}$$

from 0.077 to 0.053. The three Li positions were then readily located in a difference

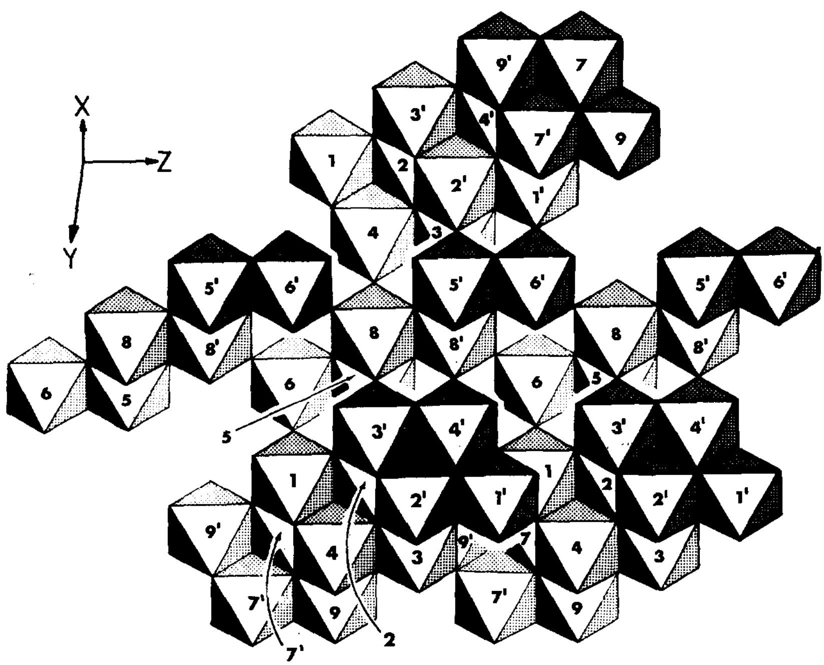

FIG. 1. The idealized structure of H-$Li_2Mo_4O_{13}$ (cf. (*2*) Fig. 2)). Octahedra numbered 1 to 6 correspond to the octahedra around Mo(1) to Mo(6), respectively, while 7, 8, and 9 correspond to the octahedra around Li(1), Li(2), and Li(3). Primes indicate centrosymmetrically related octahedra.

electron density map. Block-diagonal least-squares refinement of the full model, in which Mo was varied anisotropically and Li and O isotropically, gave $R = 0.031$ and $R_w = 0.035$. At this point all shifts were reduced to less than 0.1σ and the refinement was terminated.[1] A difference Fourier synthesis contained no features greater than ± 2.0 eÅ^{-3}. The final positional and thermal parameters are reported in Table II.

Description and Discussion

Like L-$Li_2Mo_4O_{13}$, H-$Li_2Mo_4O_{13}$ is a regular derivative structure of V_6O_{13} (*3*, *4*) (Fig. 1). Where L-$Li_2Mo_4O_{13}$ has Li and Mo separated into layers, there is no layer in H-$Li_2Mo_4O_{13}$ which contains one kind of metal only, although the metals are strictly ordered. The distribution of the metals in H-$Li_2Mo_4O_{13}$ should be clear from the z-axis projections of the L and H forms (Fig. 2).

The distortions within the Mo–O octahedra in this compound are virtually identical to those found in L-$Li_2Mo_4O_{13}$. With the values found in L-$Li_2Mo_4O_{13}$ included in parentheses, the ranges for the short, medium, long, and very long Mo–O distances are 1.67(1.67) to 1.75(1.75) Å, 1.89(1.89) to 2.04(2.04) Å, 2.12(2.13) to 2.28(2.27) Å, and 2.32(2.34) to 2.60(2.64) Å, respectively (Table III). The Li–O distances lie between 1.90(1.91) and 2.61(2.58) Å. The values found for metal–metal distances also agree quite closely with those found in the low-temperature form (*2*).

The most significant feature of this structure is its relationship to L-$Li_2Mo_4O_{13}$; a relationship which can be explained readily in terms

[1] A table of observed and calculated structure factors has been deposited as Document No. NAPS-02502 with the ASIS National Auxiliary Publications Service, c/o Microfiche Publications, 440 Park Avenue South, New York, N.Y. 10016. A copy may be secured by citing the document number and by remitting \$5.30 for photocopies or \$1.50 for microfiche. Advance payment is required. Make check or money order payable to ASIS-NAPS.

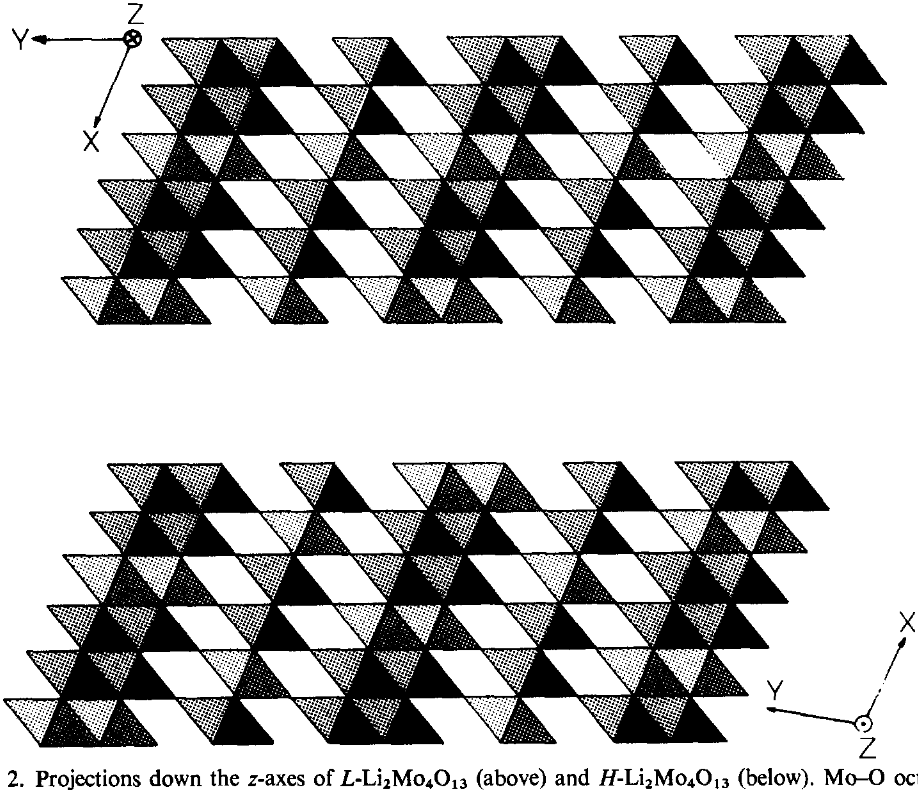

FIG. 2. Projections down the z-axes of L-$Li_2Mo_4O_{13}$ (above) and H-$Li_2Mo_4O_{13}$ (below). Mo–O octahedra have been shaded more heavily than the Li–O octahedra.

TABLE III

SELECTED INTERATOMIC DISTANCES (Å) IN H-$Li_2Mo_4O_{13}$*

Metal–metal distances

Mo–Mo edge-shared octahedra	
Mo(1)–Mo(2)	3.228(2)
Mo(1)–Mo(1′)^a	3.382(2)
Mo(1)–Mo(4)	3.492(2)
Mo(2)–Mo(3′)	3.232(2)
Mo(2)–Mo(2′)	3.509(2)
Mo(2)–Mo(3)	3.568(2)
Mo(2)–Mo(4)	3.595(2)
Mo(3)–Mo(4)	3.266(2)
Mo(5)–Mo(6)^a	3.267(2)
Mo(6)–Mo(6)^j	3.289(2)

Mo–Li edge-shared octahedra	
Mo(1)–Li(1)^h	3.21(3)
Mo(3)–Li(3′)	3.23(2)
Mo(4)–Li(3)^b	3.15(3)
Mo(4)–Li(1)^b	3.31(2)
Mo(5)–Li(2)^g	3.21(3)

Li–Li edge-shared octahedra	
Li(1)–Li(3)	3.34(4)
Li(1)–Li(3′)^i	3.45(4)
Li(1)–Li(1′)^i	3.52(4)
Li(2)–Li(2′)^c	3.44(4)

Mo–Mo corner-shared octahdera	
Mo(1)–Mo(4′)^a	3.729(2)
Mo(1)–Mo(3′)	3.943(2)
Mo(1)–Mo(6)^e	4.288(2)
Mo(2)–Mo(4′)	3.962(2)
Mo(2)–Mo(5)^c	4.252(2)
Mo(5)–Mo(5′)^k	3.771(2)
Mo(5)–Mo(6′)^k	3.962(2)

Mo–Li corner-shared octahedra	
Mo(1)–Li(3′)^a	3.67(2)
Mo(2)–Li(3′)	3.62(3)
Mo(2)–Li(1)^b	3.67(2)
Mo(3)–Li(1′)	3.55(3)
Mo(3)–Li(3)^b	3.61(3)
Mo(3)–Li(2′)	3.83(3)
Mo(4)–Li(1′)^a	3.60(3)
Mo(4)–Li(2)^g	3.96(3)
Mo(5)–Li(3)^b	3.66(2)
Mo(5)–Li(2′)	3.67(3)
Mo(6)–Li(1′)	3.59(2)
Mo(6)–Li(2′)	3.60(3)
Mo(6)–Li(2)^h	3.70(3)

Metal–oxygen distances

Mo–O octahedra

Mo(1)–O(18′)^a	1.694(9)	Mo(3)–O(7′)	1.688(8)	Mo(5)–O(8)	1.693(9)
Mo(1)–O(19)	1.696(8)	Mo(3)–O(12′)	1.718(9)	Mo(5)–O(2′)^g	1.722(8)
Mo(1)–O(17′)^a	1.925(8)	Mo(3)–O(3)	1.907(7)	Mo(5)–O(1)^g	1.886(1)
Mo(1)–O(10)	2.042(8)	Mo(3)–O(11′)	1.919(8)	Mo(5)–O(14)	1.984(8)
Mo(1)–O(11)	2.170(8)	Mo(3)–O(4)	2.280(9)	Mo(5)–O(13)	2.138(8)
Mo(1)–O(17)	2.320(7)	Mo(3)–O(5′)	2.410(8)	Mo(5)–O(6)^g	2.578(8)
Mo(2)–O(6)	1.687(8)	Mo(4)–O(9)	1.673(8)	Mo(6)–O(20′)	1.697(8)
Mo(2)–O(5′)	1.747(9)	Mo(4)–O(16)	1.717(8)	Mo(6)–O(15′)^g	1.704(9)
Mo(2)–O(4′)	1.928(7)	Mo(4)–O(3)	1.942(8)	Mo(6)–O(13′)^k	1.896(9)
Mo(2)–O(10)	1.942(8)	Mo(4)–O(17)	1.974(9)	Mo(6)–O(14)^f	1.910(8)
Mo(2)–O(11)	2.120(8)	Mo(4)–O(4)	2.164(8)	Mo(6)–O(13)^f	2.243(9)
Mo(2)–O(4)	2.522(7)	Mo(4)–O(10)	2.409(7)	Mo(6)–O(19)^h	2.602(8)

Li–O octahedra

Li(1)–O(20)	1.90(2)	Li(2)–O(15)^c	1.94(3)	Li(3)–O(8)^d	1.97(3)
Li(1)–O(12)	1.96(3)	Li(2)–O(2)^c	2.02(3)	Li(3)–O(18)	2.00(2)
Li(1)–O(16′)^a	1.97(2)	Li(2)–O(14)^c	2.06(3)	Li(3)–O(5)	2.01(3)
Li(1)–O(10)^d	2.07(3)	Li(2)–O(7)	2.14(3)	Li(3)–O(3)^d	2.01(3)
Li(1)–O(16)^d	2.50(2)	Li(2)–O(9)^c	2.30(3)	Li(3)–O(12)	2.28(2)
Li(1)–O(18′)^i	2.61(3)	Li(2)–O(2′)	2.54(3)	Li(3)–O(16)^d	2.59(3)

* Estimated standard deviations are in parentheses. The numbering of the atoms is in accordance with that in Table II, with primes indicating the equivalent position ($\bar{x}$, $\bar{y}$, $\bar{z}$). The superscripts indicate that the atom is in an adjacent unit cell, and its relationship to the primary unit cell is given by: a (0,0,−), b (−,0,0), c (0,−,0), d (+,0,0), e (0,−,−), f (0,0,+), g (0,+,0)h (0,+,+), i (+,0,−), j (−,+,+), k (−,0,+).

of movement of one of the two shear planes through the structure. Since *L*- and *H*-$Li_2Mo_4O_{13}$ are derivative structures of V_6O_{13}, they are formed by 3 × 2 columns of ReO_3-type structure joined by two perpendicular shear planes (*10*, *11*). The first shear plane runs between octahedra 1, 2, 3′, 4′, 7, and 8 (Fig. 4a) and the symmetry-related octahedra 1′, 2′, 3, 4, 7′, and 8′ and gives rise to the double sheet of octahedra which can be seen in the diagram. The second shear plane, which is relevant to the following discussion, runs between octahedra 1′, 3′, and 8 and 2, 4′, and 7, between octahedra 4, 2′, and 7′ and 3, 1′, and 8′ and between octahedra 5′, 6, and 9′ and 6′, 5, and 9.

The sheet of octahedra 1, 2, 3′, 4′, 7, and 8 (Fig. 4a) is identical to those formed by 3, 4, 1′, 2′, 7′, and 8′ and 5′, 6′, 5, 6, 9, and 9′.

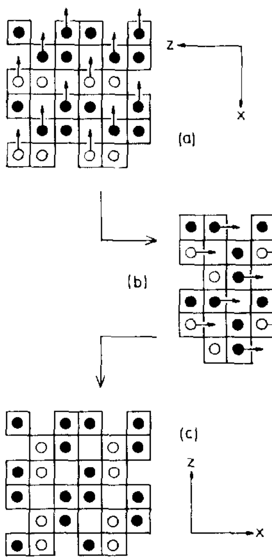

FIG. 3. The relationship between *L*-$Li_2Mo_4O_{13}$ and *H*-$Li_2Mo_4O_{13}$ in two dimensions. (a) represents a single sheet of octahedra in *L*-$Li_2Mo_4O_{13}$. Filled circles denote Mo–O octahedra, open circles represent Li–O octahedra. The first step in the movement of the shear plane occurs when half of the metals and the associated apical oxygens (above and below the plane) move into adjacent vacant sites as shown. The oxygens move into the cube-octahedral holes in the structure in order to retain octahedral coordination about the molybdenums. (b) The shear plane moves again when the atoms move once more into sites which were vacated in the first movement to give (c).

Therefore, it is simpler to show first the movement of the shear plane in this sheet only (Fig. 3). The first movement of the shear plane results in a structure called, for convenience, the "intermediate form." The second movement results in a structure in which the planes of Li and Mo are perpendicular to those in the original structure. On examining the three-dimensional structure, one can see that the planes of metal atoms no longer contain either Mo or Li only, but that the structure is actually *H*-$Li_2Mo_4O_{13}$ where any one plane contains both Li and Mo. This process is shown for the whole structure in Fig. 4.

Brower and co-workers (*1*) have stated that *H*-$Li_2Mo_4O_{13}$ is the stable polymorph and that *L*-$Li_2Mo_4O_{13}$ is actually a metastable polymorph. It can be shown, at least qualitatively, that this is probably correct. Since the *H*- and *L*-forms are derivatives of the same structure with the number and lengths of Mo–Mo, Mo–Li, Li–Li, Mo–O, and Li–O distances being virtually the same in both polymorphs, then, to a first approximation, all factors which determine the stability of the phase will be the same with the exception of the electrostatic repulsion between the metals in the double and single sheets of octahedra in the structure (Fig. 2). It can be shown by a simple calculation that these repulsions are probably between 0.5% and 1% higher in *L*-$Li_2Mo_4O_{13}$ than in *H*-$Li_2Mo_4O_{13}$ and, therefore, that the *H*-form is probably the most stable polymorph.

It has been found that melts cooled at a rate of between 5 and 10 deg/hr and reaction of Li_2CO_3 or Li_2MoO_4 and MoO_3 below the melting point for up to 2 days always yields the low-temperature (metastable) form. It would seem that the nature of the species reacting is such that *L*-$Li_2Mo_4O_{13}$ is the kinetically favored form. It may be that *H*-$Li_2Mo_4O_{13}$ is only formed via *L*-$Li_2Mo_4O_{13}$ and that the mechanism of the transformation is the movement of the shear plane mentioned above. In this case the transformation would be reconstructive with a high activation energy and would require the *L*-form to be heated to high temperatures for long periods of time in order for the transformation to take

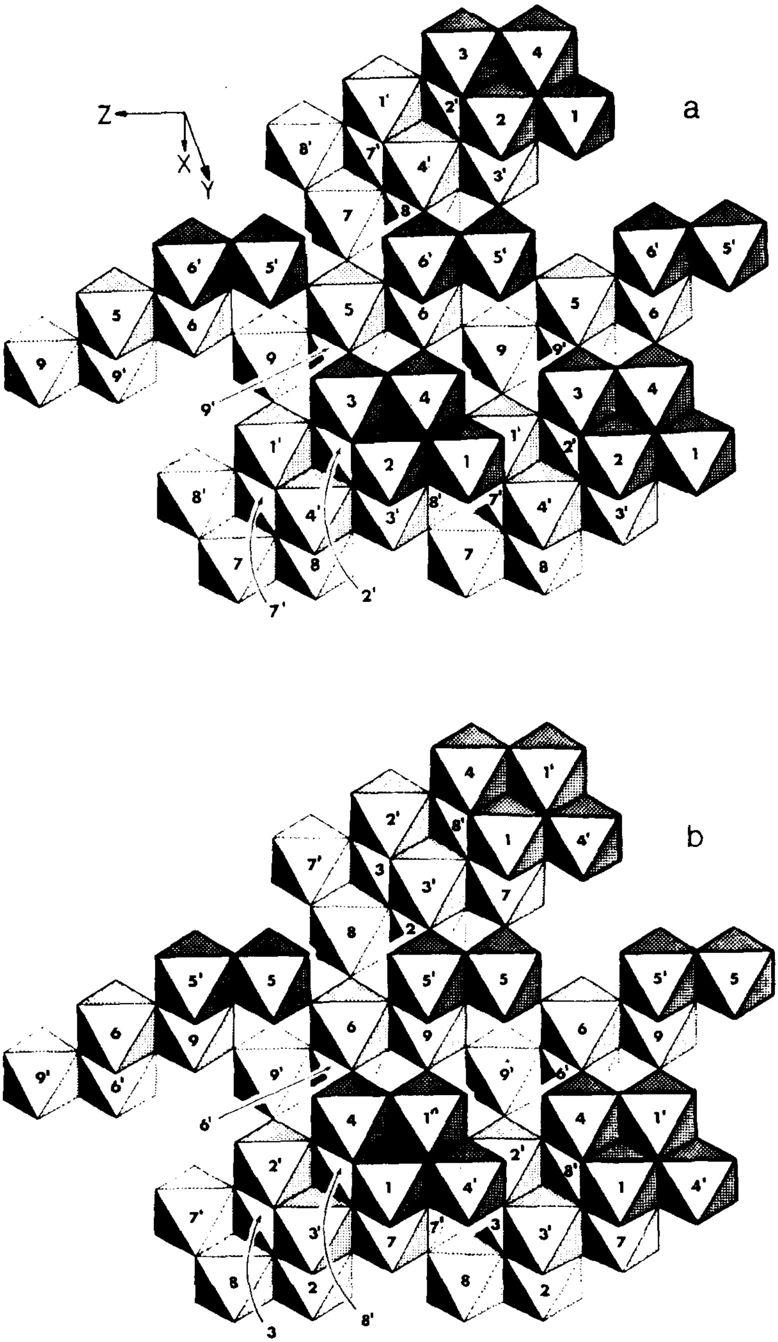

FIG. 4. The relationship between L-$Li_2Mo_4O_{13}$ and H-$Li_2Mo_4O_{13}$ in three dimensions. (a) shows L-$Li_2Mo_4O_{13}$ numbered as in (*2*). (b) shows the "intermediate" formed after the first movement of the shear plane (Fig. 3). (c) is a diagram of the final structure, H-$Li_2Mo_4O_{13}$. The numbering is consistent with that of L-$Li_2Mo_4O_{13}$. To compare this with H-$Li_2Mo_4O_{13}$ (Fig. 1) the numbers 1 to 9 should be replaced by 3′, 4′, 1′, 2′, 6′, 5′, 7, 9′, 8′, respectively.

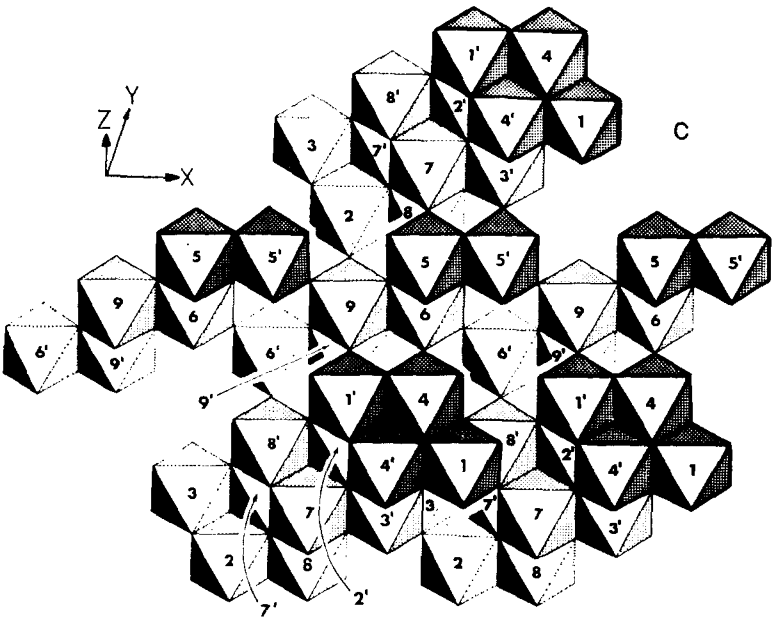

FIG. 4—*continued.*

place. This appears to be consistent with the results of Brower et al. (*1*).

Monoclinic Lithium Tetramolybdate

During this study two unusual crystals, both of which have since decomposed, were found in a melt preparation of L-$Li_2Mo_4O_{13}$. Weissenberg and precession photography showed that this compound was monoclinic with space group $P2_1$ or $P2_1/m$. The $hk0$ and $0kl$ photographs are remarkably similar to those of H- and L-$Li_2Mo_4O_{13}$ (apart from a doubling of $d_{(010)}$). This similarity is reflected in the dimensions a, c and β of the three compounds (Table IV) and $d_{(010)}$ for the H- and L-forms, which is 10.69 Å, while $d_{(020)}$ for the monoclinic compound is 10.705 Å. Because of these similarities it seems reasonable to assume that this compound is probably another metastable polymorph of $Li_2Mo_4O_{13}$ (henceforth denoted M-$Li_2Mo_4O_{13}$) based on a shear structure similar to V_6O_{13}. However, V_6O_{13} is not consistent with the space groups $P2_1$ or $P2_1/m$, at least in this orientation, since the 2_1 axis causes every second double sheet of octahedra to be inverted. It follows that M-$Li_2Mo_4O_{13}$ cannot be the "intermediate form" mentioned previously.

Summary

Both H-$Li_2Mo_4O_{13}$ and metastable L-$Li_2Mo_4O_{13}$ are derivative structures, or superstructures, of V_6O_{13}, a structure derived from ReO_3 by two perpendicular shearing operations which give rise to 3 × 2 columns of corner-sharing octahedra joined at shear

TABLE IV

CRYSTALLOGRAPHIC DATA FOR THE POLYMORPHS OF $Li_2Mo_4O_{13}$

	M	*H*	*L*
Symmetry	Monoclinic	Triclinic	Triclinic
Space group	$P2_1/m$ or $P2_1$	$P\bar{1}$	$P\bar{1}$
a (Å)	8.600(4)	8.612(4)	8.578(5)
b (Å)	21.41(1)	11.562(6)	11.450(5)
c (Å)	8.220(4)	8.213(4)	8.225(5)
α (deg.)	90	94.45(7)	109.24(7)
β (deg.)	96.27(7)	96.38(7)	96.04(7)
γ (deg.)	90	111.24(7)	95.95(7)
V (Å^3)	1504(2)	751(1)	750(1)
Z	6	3	3

planes. The two polymorphs can be related by movement of one of the two shear planes, a process which may also describe the mechanism of the $L \rightarrow H$ transformation. A monoclinic polymorph also exists and its cell dimensions and space group suggest that its structure may be based on a shear structure containing 3×2 columns of ReO_3-type corner-linked octahedra.

Acknowledgment

This work forms part of a project supported by the Australian Research Grants Committee. One of us (B.K.M.) acknowledges the receipt of a Commonwealth Postgraduate Research Award.

References

1. W. S. Brower, H. S. Parker, R. S. Roth, and J. L. Waring, *J. Cryst. Growth* **16**, 115 (1972).
2. B. M. Gatehouse and B. K. Miskin, *J. Solid State Chem.* **9**, 247 (1974).
3. F. Aebi, *Helv. Chim. Acta* **31**, 9 (1948).
4. K. A. Wilhelmi, K. Waltersson, and L. Kihlborg, *Acta Chem. Scand.* **25**, 2675 (1971).
5. D. T. Cromer and J. T. Waber, *Acta Crystallogr., Sect, B* **18**, 104 (1965).
6. W. R. Busing, K. O. Martin, and H. A. Levy, ORFLS, a Fortran Crystallographic Least-squares Program, ORNL-TM-305, Oak Ridge National Laboratory, Tennessee, 1962.
7. R. Shiono, Block-Diagonal Least-Squares Refinement Program, Department of Crystallography, University of Pittsburgh, 1968.
8. J. C. B. White, Melbourne University Fourier Summation Program MUFR3. See J. S. Rollet, *in* "Computing Methods and the Phase Problem in X ray Crystal Analysis" (R. Pepinsky, Robertson, J. M. and Speakman, J. C., Eds.), p. 87, Pergamon Press, Oxford, 1961.
9. B. M. Gatehouse and P. Leverett, *J. Solid State Chem.* **1**, 484 (1970).
10. S. Andersson, *Bull. Soc. Chim.* 1088 (1965).
11. S. Andersson, *Ark. Kemi* **26**, 521 (1967).